Supporting Information

A Phosphate Semiconductor-induced Built-in Electric Field Boosts Electrons Inspissation for Electrocatalytic Hydrogen Evolution in Alkaline

Zichuang Li,[ad] Yu Pei,[ab] Ruguang Ma,*[ab] Yuandong Wang,[ab] Yufang Zhu,*[ac] Minghui Yang[e] and Jiacheng Wang*[ab]

[a.] State Key Laboratory of High-Performance Ceramics and Superfine Microstructure, Shanghai Institute of Ceramics, Chinese Academy of Sciences, 1295 Dingxi Road, Shanghai 200050, China. E-mail: jiacheng.wang@mail.sic.ac.cn; maruguang@mail.sic.ac.cn.

[b.] Center of Materials Science and Optoelectronics Engineering, University of Chinese Academy of Sciences, 100049 Beijing, China

[c.] Hubei Key Laboratory of Processing and Application of Catalytic Materials, College of Chemical Engineering, Huanggang Normal University, Huanggang City, Hubei Province 438000, China. Email: zjf2412@163.com

[d.] School of Materials Science and Engineering, University of Shanghai for Science and Technology, 516 Jungong Road, Shanghai 200093, China.

[e.] Ningbo Institute of Materials Technology and Engineering Chinese Academy of Sciences, 1219 Zhongguan West Road, Ningbo 315201, China

Experimental Procedures

Chemicals

Bi(NO$_3$)$_3$· 5H$_2$O, NaH$_2$PO$_2$· H$_2$O, and NaOH were purchased from Sinopharm Chemical Reagent Co. Ltd. RuCl$_3$ · xH$_2$O (35.0% - 42.0% Ru basis, Aladdin), and N-methylpyrrolidone (NMP) were purchased from Aladdin. All chemicals used are analytical regents (AR).

Materials synthesis

Firstly, RuCl$_3$ (0.5 mmol) and Bi(NO$_3$)$_3$· 5H$_2$O (0.25 mmol) were dissolved in NMP, followed by the addition of acetylene black (0.3 g). NaOH (0.20 g in 10 mL NMP) was slowly added into the above mixture with stirring at 50 ℃, and the mixture was kept at 50 ℃ for 20 h under stirring. Then, the solid was collected by suction filtration, followed by drying to obtain the precursor Ru-Bi-O. Finally, Ru-Bi-O (0.1 g) was put in a tube furnace and NaH$_2$PO$_2$· H$_2$O (0.3 g) was placed above the gas flow. Then the sample was maintained at 300 °C for 2 h under an Ar atmosphere. By changing the feed ratio, Ru/BiPO$_4$-1:1 and Ru/BiPO$_4$-3:1 can be obtained in the same way. Similarly, BiPO$_4$ was synthesised through same process without RuCl$_3$. And Ru/C was synthesised without Bi(NO$_3$)$_3$· 5H$_2$O and heading at 5% H$_2$ in Ar to replace Ar and NaH$_2$PO$_2$· H$_2$O.

Electrochemical measurements

The electrochemical measurements were carried out with an electrochemical work station (CHI 760E, Shanghai Chenhua, China) in a conventional three-electrode cell system at room temperature with a graphite rod as the counter electrode, an Hg/HgO electrode as the reference electrode, and a commercial glassy carbon electrode (GCE, 5 mm diameter, 0.196 cm^2) as the working electrode. The Hg/HgO electrode was experimentally calibrated against RHE. The presented current density referred to the geometric surface area of the GCE. The electrolyte was a 1 M or 3 M KOH aqueous solution. The working electrodes were prepared as follows: 5 mg material and 20 μL Nafion solution (5 wt.%) were ultrasonically dispersed in 1 mL

water/ethanol (vol: vol, 1:1) solution to form a homogeneous ink. The electrocatalyst suspension (20 μL) was loaded onto GCE (0.196 cm^2) as the working electrode and then dried in an oven at 50 ℃. The potential, measured against a Hg/HgO electrode, was converted to the potential versus the reversible hydrogen electrode (RHE) according to the following equation:

$$E \text{ (vs. RHE)} = E \text{ (vs. Hg/HgO)} + 0.095 \text{ V} + 0.0591*pH \tag{1}$$

Linear sweep voltammetry (LSV) curve was corrected by 90% IR. Electrochemical impedance spectroscopy measurements were carried out by applying an a.c. voltage with 10 mV amplitude in a frequency range from 1 Hz to 1 MHz at a potential of -1.2 V. The electrochemically active surface area of samples was estimated from the slope of the C_{dl} value. Cyclic voltammetry (CV) was measured at a scan rate of 20 mV s^{-1} ~ 180 mV s^{-1} in the voltage window from -0.955 V to -0.755 V. The Tafel slopes were obtained from the treatment of the polarization curve based on the Tafel equation:

$$\eta = a + b \log j \tag{2}$$

where η is the overpotential, a is the intercept, b is the Tafel slope and j is the current density.

Structural characterization

Powder X-ray diffraction (XRD) analysis was performed using a D8 ADVANCE instrument with Cu Kα1 radiation (40 kV, 60 mA). Scanning electron microscopy (SEM) images were recorded using a field emission scanning electron micro-analyzer (FEI Magellan 400), and transmission electron microscopy (TEM) images were obtained using a JEM-2100F. To analyze the surface of the samples, X-ray photoelectron spectroscopy (XPS) measurements were taken using an ESCALAB 250 X-ray photoelectron spectrometer using Al Kα (hν = 1486.6 eV) radiation. Ultraviolet photoelectron spectroscopy (UPS) was obtained from Thermo Fisher Nexsa XPS. Electron paramagnetic resonance (EPR) was recorded on Bruker EMX

spectrometer using an Elexsys probe head. Calculation of the spin number was based on a reference powder of Cu(II)TPP with 1 spin per molecule.

Calculation details

All DFT calculations were performed using the Vienna ab initio simulation package (VASP).[1-2] The generalized gradient approximation method with the Perdew–Burke–Ernzerhof (PBE)[3] exchange–correlation functional was used to manage the electron exchange and correlation energy. The plane wave basis (kinetic energy cut-off value was 450 eV was employed to describe the valence electrons. A mesh of $2 \times 2 \times 1$ was used for the k-point sampling obtained from the Gamma center. Meanwhile, the model of Ru/BiPO$_4$ is $13.73 \times 12.68 \times 30$ Å^3, the thickness of the vacuum layer is 20 Å. The atomic positions were fully optimized until the energy and forces are converged to 1×10^{-5} eV and 0.0257 eV Å^{-1}, respectively. For TS calculation, the parameters of CI-NEB are kept the same as the structure relaxation. Three transition states are inserted between initial state and final state using VASPKIT package. The calculations of binding energy of HER intermediates were conducted following method which was used by Nørskov:[4]

$$\Delta G = \Delta E + \Delta ZPE - T\Delta S \tag{3}$$

$$\Delta E = E_{(H*)} - E_{(*)} - E_{(H)} \tag{4}$$

Note: * is catalyst, H* is adsorbed H, $E_{(H)} = 1/2\ E_{(H2)}$

The values of ΔZPE and TΔS are referred in the other work.[4]
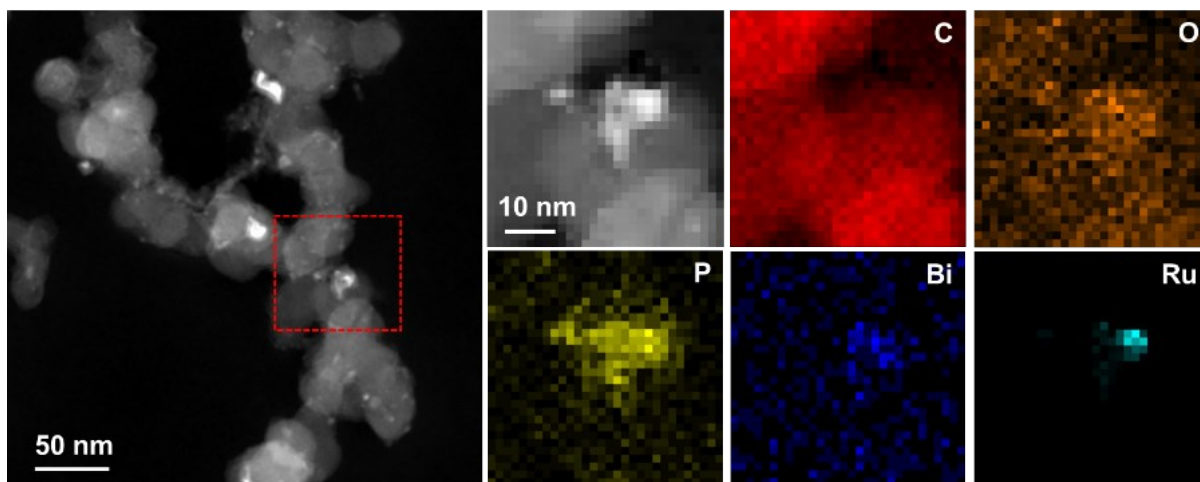
Figure S1. The TEM elemental mappings images of Ru/BiPO$_4$.
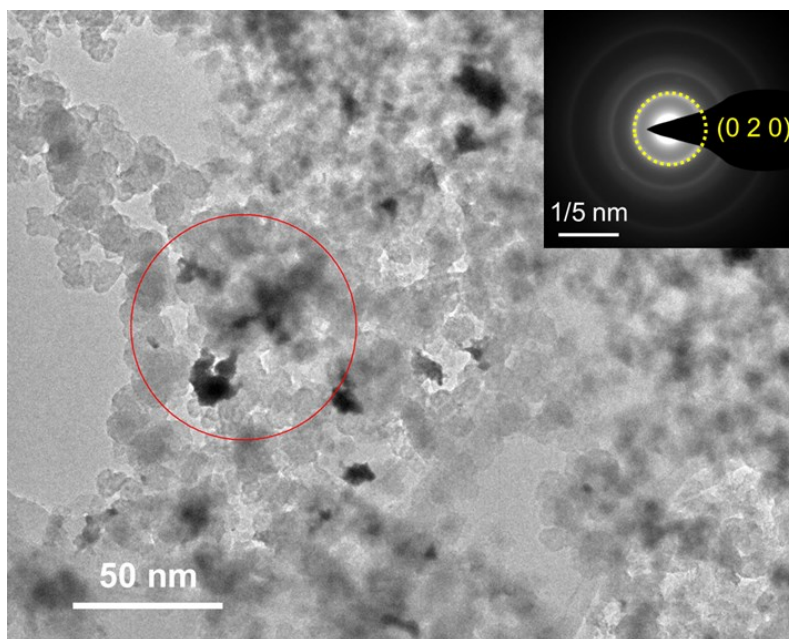
Figure S2. The selected area electron diffraction results of Ru/BiPO$_4$.
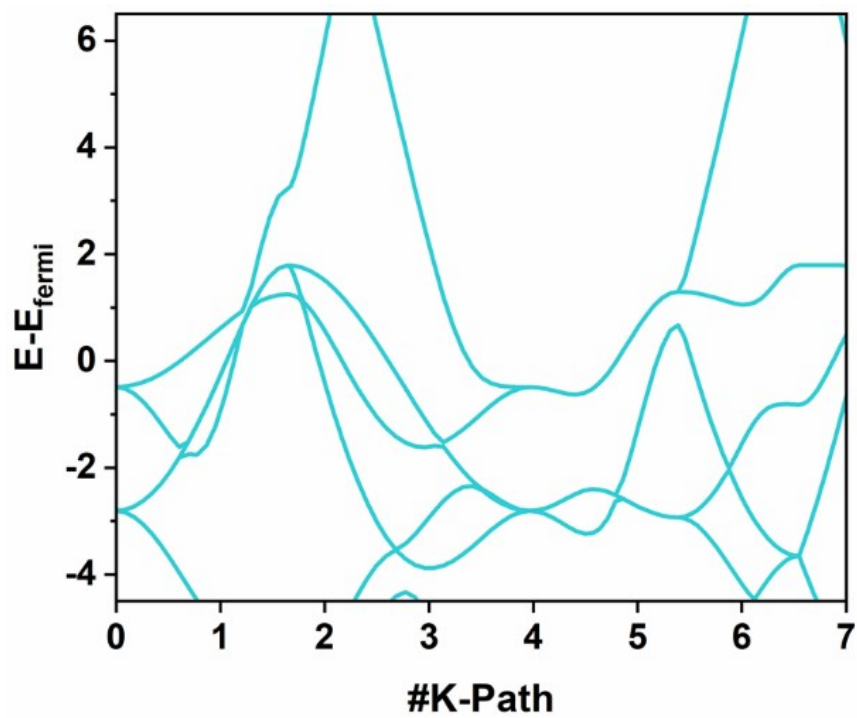
Figure S3. The band structure of Ru.
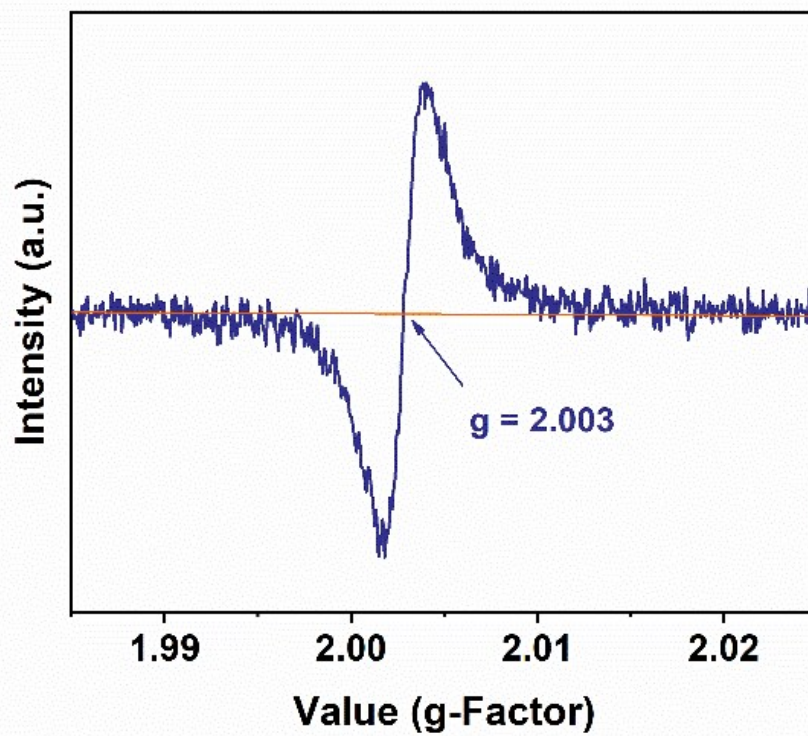
Figure S4. The electron paramagnetic resonance spectra of BiPO$_4$.
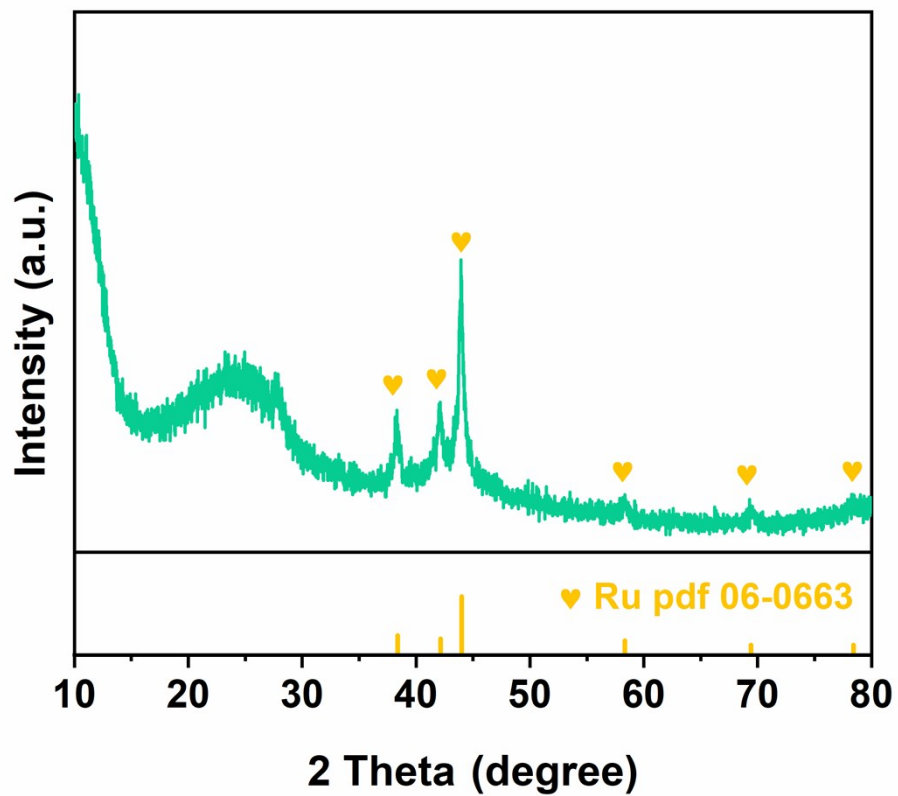
Figure S5. The X-ray diffraction pattern of Ru/C.
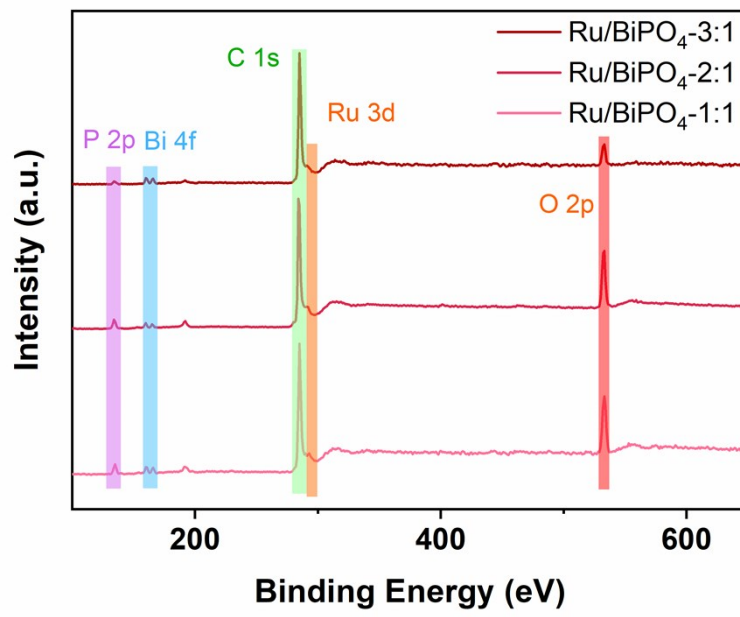
Figure S6. The full XPS spectrum of Ru/BiPO$_4$-1:1, Ru/BiPO$_4$ and Ru/BiPO$_4$-3:1.
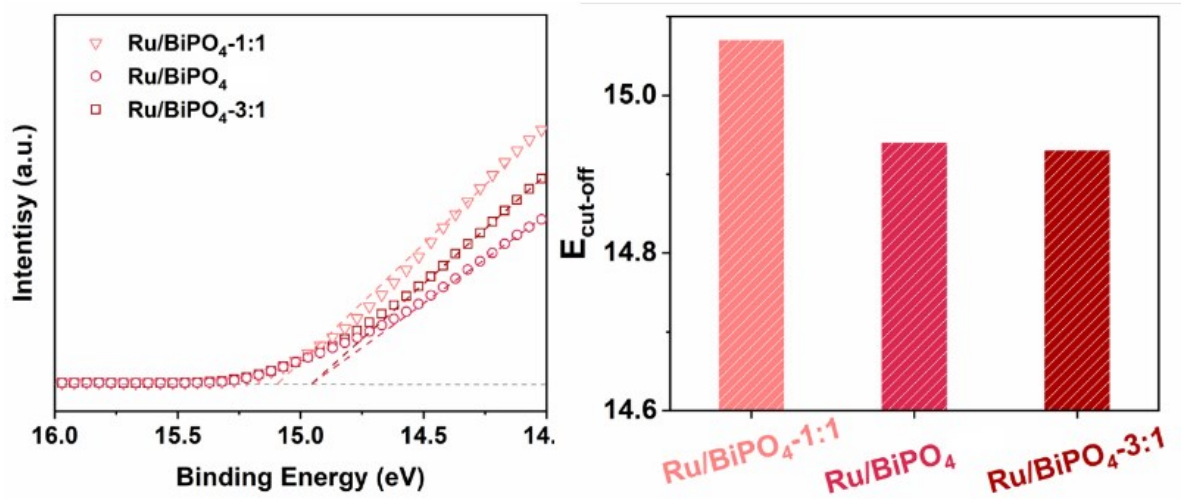
Figure S7. The Ecut-off of $Ru/BiPO_4$-1:1, $Ru/BiPO_4$ and $Ru/BiPO_4$-3:1.
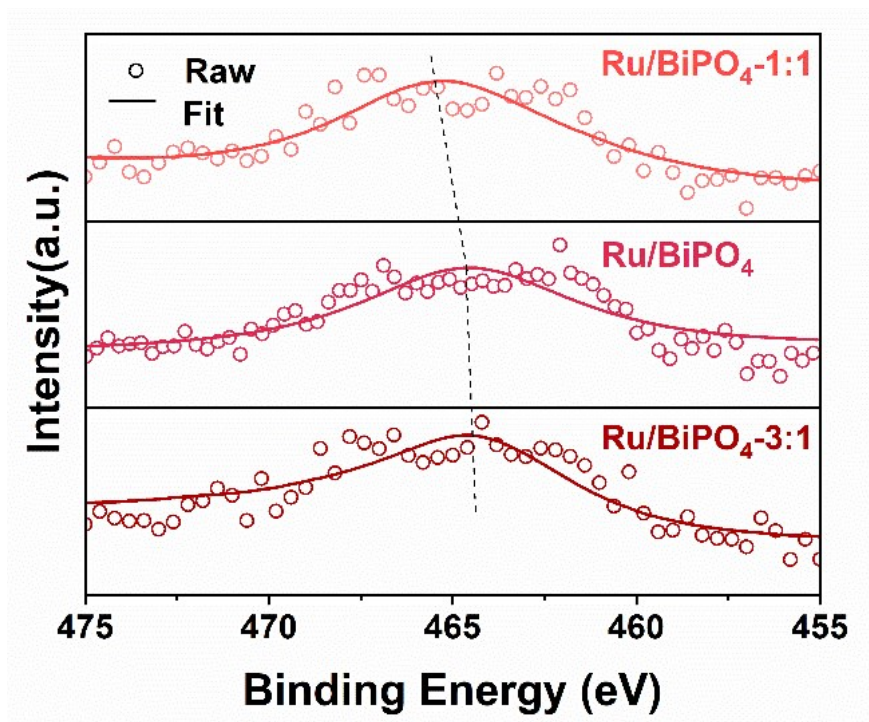
Figure S8. The High-resolution XPS spectra for Ru 3p for Ru/BiPO$_4$-1:1, Ru/BiPO$_4$ and Ru/BiPO$_4$-3:1.
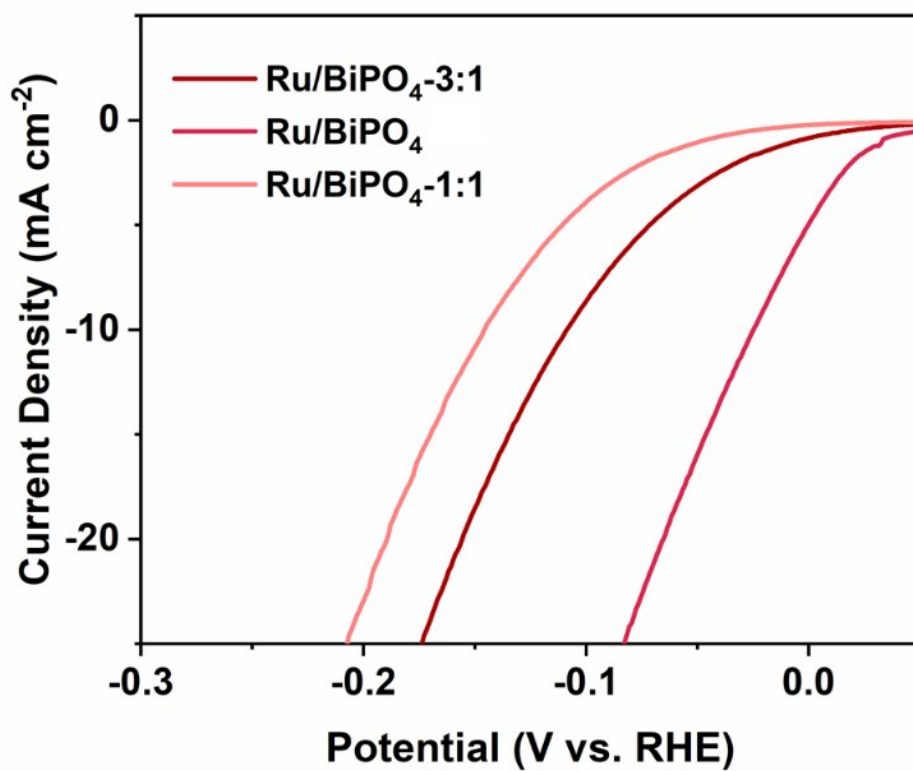
Figure S9. The LSV curves of Ru/BiPO$_4$-1:1, Ru/BiPO$_4$ and Ru/BiPO$_4$-3:1.
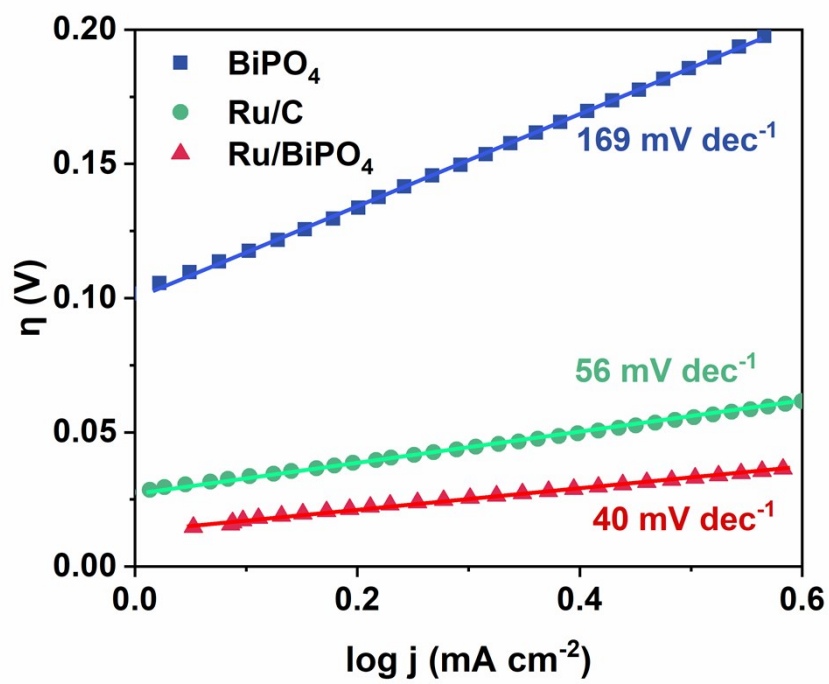
Figure S10. The Tafel slopes of $BiPO_4$, Ru/C and Ru/$BiPO_4$.
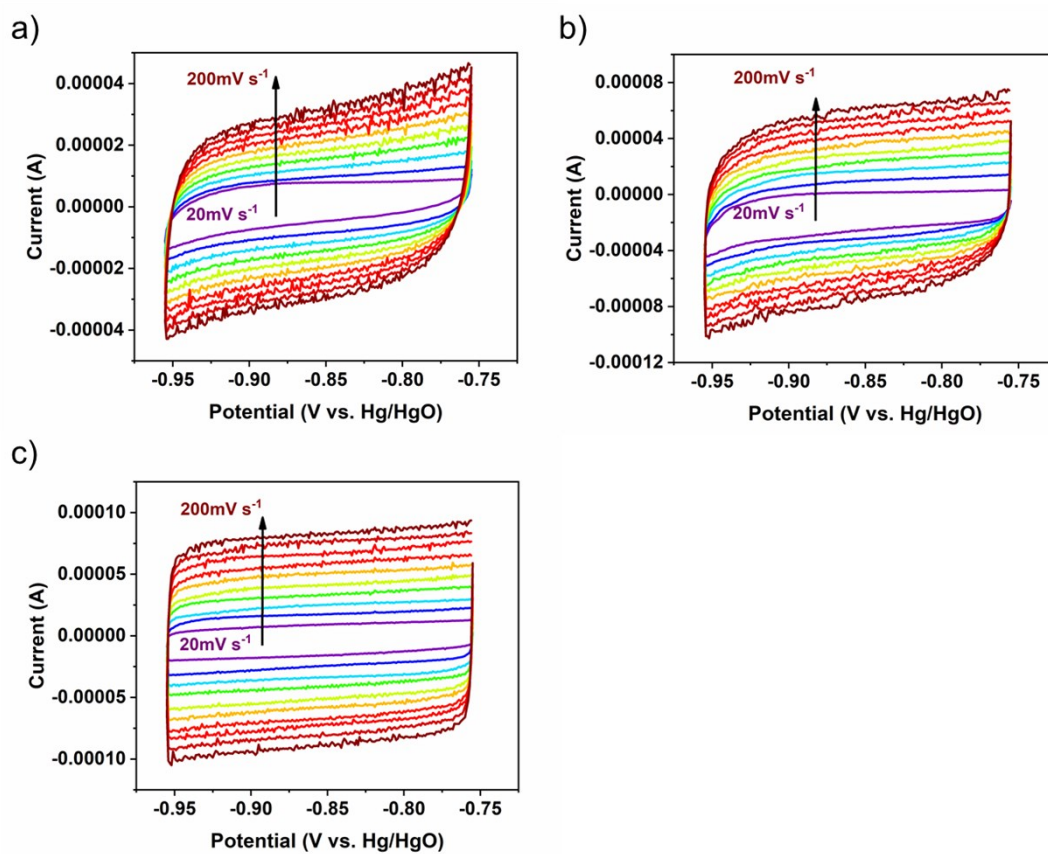
Figure S11. The scanning CV curves of a) $BiPO_4$, b) Ru/C and c) $Ru/BiPO_4$.
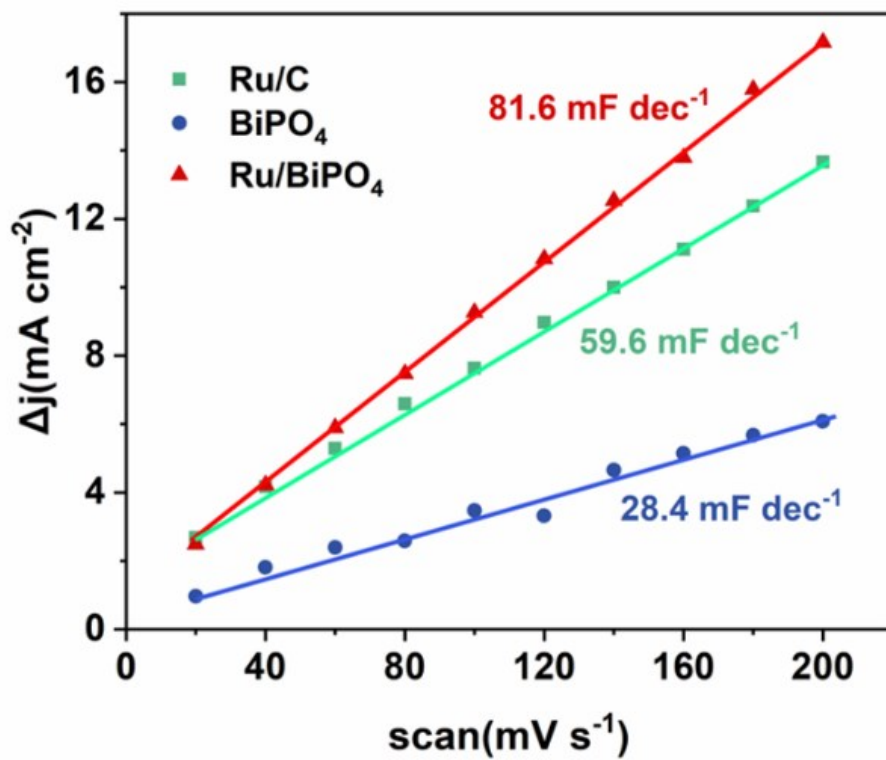
Figure S12. The ECSA of BiPO$_4$, Ru/C and Ru/BiPO$_4$.
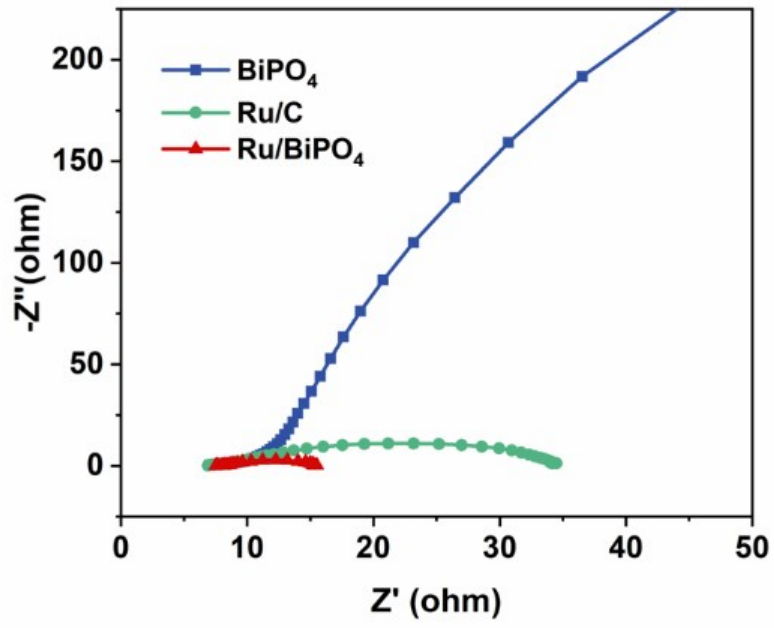
Figure S13. The EIS of $BiPO_4$, Ru/C and Ru/$BiPO_4$.
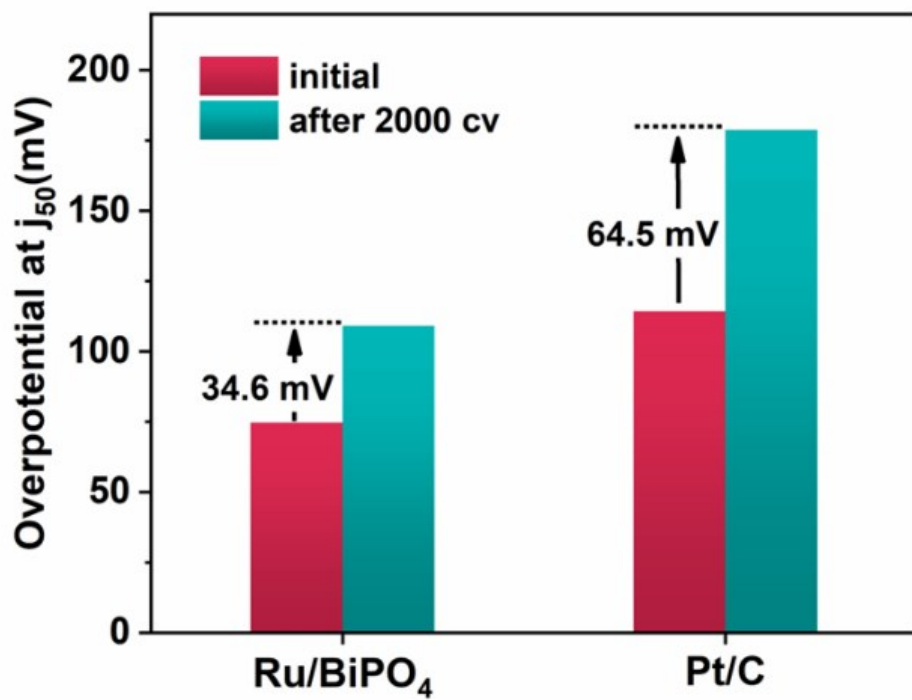
Figure S14. The stability of Pt/C and Ru/BiPO$_4$ in 3 M KOH.
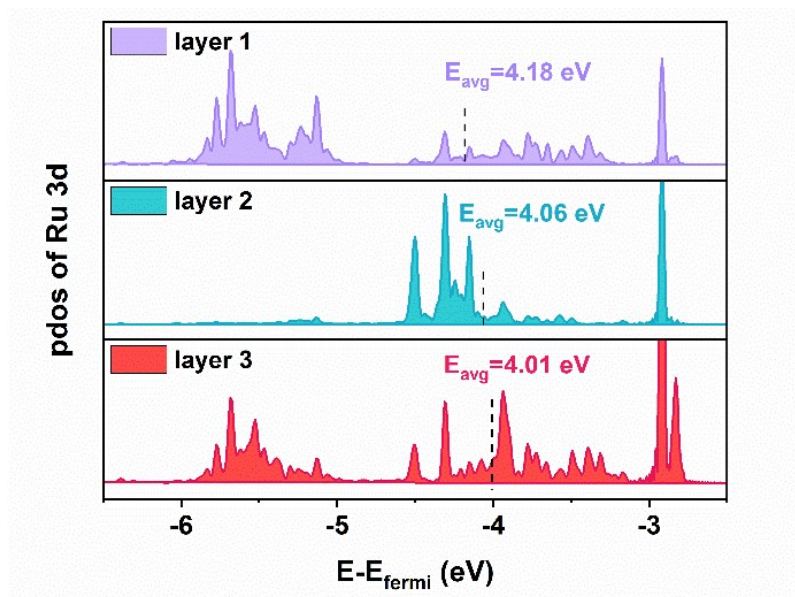
Figure S15. The pDOS of Ru 3d for each layer of Ru cluster in Ru/BiPO$_4$.

Table S1. The elemental contents in Ru/BiPO$_4$-X, Ru/C and Pt/C

	Ru (wt.%)	Bi (wt.%)	P (wt.%)	O (wt.%)	C (wt.%)	Pt (wt.%)
Ru/BiPO$_4$-1:1	8.03	14.15	7.87	16.38	53.57	-
Ru/BiPO$_4$	10.29	13.28	7.26	16.14	53.02	-
Ru/BiPO$_4$-3:1	11.67	13.78	8.31	16.1	50.14	-
Ru/C	10.4	-	-	-	89.6	-
Pt/C	-	-	-	-	60	40

Table S2. The TOF with different Ru-based HER electrocatalyst

Samples	j at η_{10} (mA cm^{-2})	TOF (s^{-1})	Ref.
Ru/BiPO$_4$	17	3.67	This work
Ru@CQDs480	19	1.85	[5]
Ni$_5$P$_4$-Ru	10	0.99	[6]
Ni@Ni$_2$P-Ru	15	0.10	[7]
RuP$_2$@NPC	17	0.28	[8]
Ru-NC-700	11	1.04	[9]
Ru@GnP	30	0.61	[10]
Co-sub Ru	80	0.32	[11]
Cu@Ru/C	5	0.07	[12]
RuAu-0.2	37	0.17	[13]
Ru@NC(-0.2)	4.8	0.91	[14]
RuSx/S–GO	10	0.09	[15]

Table S3. The dissociation energy of water molecule.

Sites	* (eV)	*H$_2$O (eV)	TS (eV)	[H-OH]* (eV)
P in BiPO$_4$	-641.49	-656.15	-655.16	-656.09
Ru in Ru/C	-855.42	-869.97	-869.01	-870.47
P in Ru/BiPO$_4$	-687.52	-702.35	-702.02	-702.53
Ru in Ru/BiPO$_4$	-687.52	-702.17	-	-

Table S4. The Gibbis Free Energy of HER

Sites	* (eV)	*H (eV)	ΔGH (eV)
layer 1 in Ru/BiPO$_4$	-687.52	-691.37	-0.41
layer 2 in Ru/BiPO$_4$	-687.52	-691.26	-0.30
layer 3 in Ru/BiPO$_4$	-687.52	-691.08	-0.12
Ru/C	-855.42	-859.08	-0.22
BiPO$_4$	-641.49	-643.64	1.29

Structural models and atomic coordinates of all intermediates for DFT studies

Ru/C
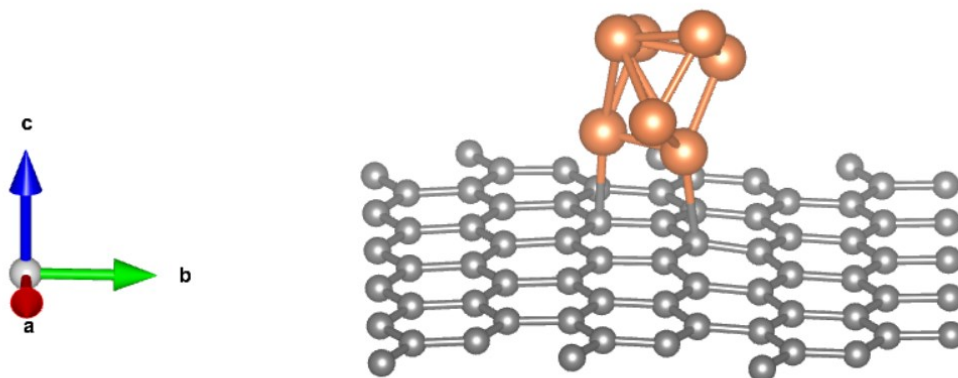
The lattice vector (Å) of the structural model.

a	12.4	0.0	0.0
b	0.0	12.6	0.0
c	0.0	0.0	30.0

Table S4. Atomic coordinates for pristine for Ru/C

-0.00148301	0.008849068	0.031469149	C
0.098262761	0.175539336	0.035659635	C
-0.00161897	0.120285739	0.034176074	C
0.098073878	0.287116482	0.036789567	C
0.198361679	0.008742245	0.031609609	C
0.298086026	0.175126909	0.036845120	C
0.198155872	0.120120576	0.034752278	C
0.297062354	0.286542258	0.039328269	C
0.398511548	0.008932942	0.031572721	C
0.498700657	0.174800760	0.037050059	C
0.398426187	0.119868964	0.035010656	C
0.499228242	0.286196176	0.040475000	C
0.598652895	0.008740778	0.031545097	C
0.698694832	0.175409406	0.035989307	C
0.598736090	0.119919423	0.034882169	C
0.698971616	0.286946074	0.038230500	C
0.798645609	0.008811763	0.031336883	C
0.898492907	0.175564065	0.035347621	C
0.798571994	0.120303554	0.034199859	C
0.898496471	0.287135137	0.036594657	C
-0.001615519	0.342500663	0.036183293	C
0.098534265	0.508983293	0.033251109	C

-0.001431197	0.453770717	0.034457258	C
0.098600488	0.620256806	0.030706113	C
0.197677573	0.342602002	0.037656871	C
0.297710732	0.509741333	0.035813271	C
0.198060880	0.453938952	0.035431490	C
0.298405150	0.620587493	0.032297713	C
0.397983052	0.342403549	0.040962627	C
0.599424046	0.342171223	0.040360132	C
0.699669489	0.509861813	0.036175813	C
0.699034894	0.620607605	0.032331416	C
0.798878491	0.342574231	0.037378468	C
0.898890737	0.509162162	0.033648271	C
0.799109647	0.454119253	0.036010670	C
0.898765030	0.620227388	0.030869456	C
-0.001253746	0.675376056	0.029568904	C
0.098598481	0.842057541	0.028681586	C
-0.001365746	0.786751798	0.028518171	C
0.098470293	0.953600854	0.030217933	C
0.198560359	0.675512089	0.030001114	C
0.298488218	0.842313044	0.028813279	C
0.198570639	0.786909665	0.028654863	C
0.298377874	0.953624441	0.030253587	C
0.498546171	0.842360636	0.029033931	C
0.398522857	0.787185870	0.029177058	C
0.498604552	0.953652375	0.030264121	C
0.698803353	0.842197292	0.028699960	C
0.598707355	0.787139869	0.029044323	C
0.698714444	0.953587283	0.030088996	C
0.798799107	0.675436505	0.030053049	C
0.898657216	0.842072207	0.028602464	C
0.798740936	0.786898783	0.028600403	C
0.898590537	0.953596926	0.030117055	C
0.397198016	0.455079521	0.040376168	C
0.599879040	0.454362154	0.040532371	C
0.398525668	0.676173541	0.031589428	C
0.598764403	0.676238920	0.031449738	C
0.498686280	0.622319225	0.034433200	C
0.498646865	0.511177888	0.040633322	C
0.667289345	0.433601267	0.159275038	Ru
0.527207134	0.489823957	0.115925550	Ru
0.605900144	0.520553949	0.220003782	Ru
0.446268824	0.557904477	0.178603433	Ru
0.317723948	0.412738682	0.173642127	Ru
0.415627463	0.349692917	0.114068221	Ru
0.490877871	0.375981024	0.198618929	Ru

25
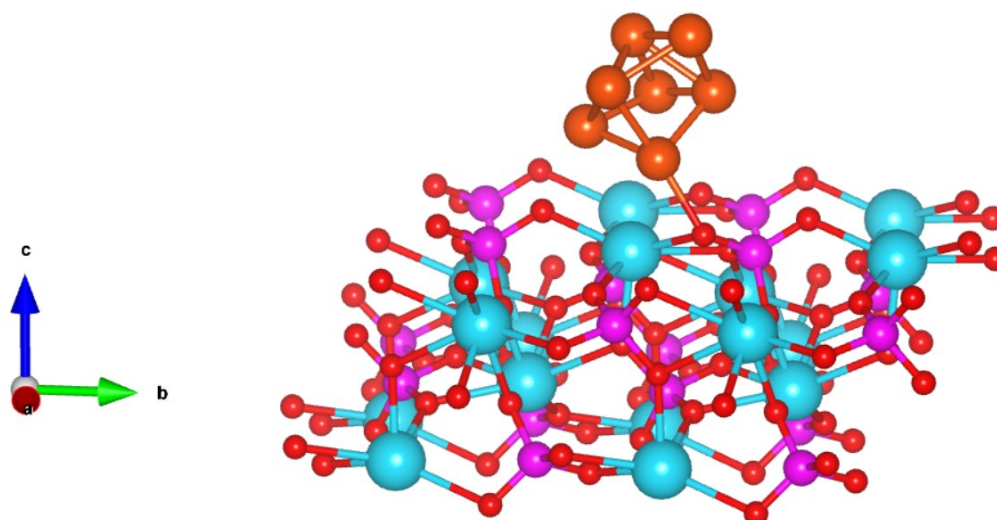
Ru/BiPO$_4$

The lattice vector (Å) of the structural model.

a	13.7	0.0	0.0
b	3.2	12.7	0.0
c	0.0	0.0	30.0

Table S5. Atomic coordinates for pristine for Ru/BiPO$_4$

0.106959993	0.292569983	0.083633359	Bi
0.356960013	0.042569996	0.033526675	Bi
0.393310039	0.204939996	0.147513358	Bi
0.143360011	0.488999983	0.193946679	Bi
0.606959958	0.292569983	0.083633359	Bi
0.856959944	0.042569996	0.033526675	Bi
0.893299827	0.204939996	0.147520002	Bi
0.643359993	0.488999983	0.193946679	Bi
0.106959979	0.792569994	0.083633359	Bi
0.356960001	0.542569998	0.033526675	Bi
0.393299982	0.704940026	0.147520002	Bi
0.143370013	0.989000013	0.193946679	Bi
0.606959979	0.792569994	0.083633359	Bi
0.856959967	0.542569998	0.033526675	Bi
0.893299818	0.704930024	0.147513358	Bi
0.643369944	0.989000013	0.193946679	Bi
0.101090001	0.055829995	0.079606628	P
0.351090013	0.305829996	0.037553342	P
0.403189990	0.454919987	0.150979996	P
0.146649996	0.220249991	0.196239980	P

0.601089897	0.055829995	0.079606628	P
0.851089908	0.305829996	0.037553342	P
0.903190025	0.454910022	0.150979996	P
0.646659999	0.220249991	0.196239980	P
0.101089986	0.555830011	0.079606628	P
0.351089999	0.805830007	0.037553342	P
0.403190006	0.954920017	0.150979996	P
0.146649987	0.720240018	0.196239980	P
0.601089986	0.555830011	0.079606628	P
0.851089999	0.805830007	0.037553342	P
0.903189999	0.954909939	0.150979996	P
0.646659991	0.720240018	0.196239980	P
0.124399982	0.471780009	0.117853292	O
0.369720037	0.220100005	0.001059977	O
0.375360069	0.035980001	0.110753314	O
0.129700005	0.322189970	0.223359998	O
0.060910005	0.008830000	0.037660027	O
0.310909997	0.258830008	0.079500008	O
0.454730034	0.515120008	0.183979988	O
0.186259987	0.243439991	0.148379993	O
0.022770000	0.158970001	0.097186661	O
0.270060013	0.408539987	0.023053360	O
0.475050032	0.347879986	0.135713323	O
0.226560027	0.124389994	0.214593315	O
0.192020027	0.103270000	0.069726690	O
0.442020009	0.353269978	0.047433345	O
0.312030011	0.417739973	0.169446659	O
0.050429998	0.174409995	0.191160011	O
0.624400070	0.471769969	0.117853292	O
0.869719967	0.220100005	0.001059977	O
0.875360183	0.035969998	0.110753314	O
0.629700177	0.322200011	0.223359998	O
0.560909987	0.008830000	0.037660027	O
0.810910046	0.258819987	0.079500008	O
0.954729984	0.515100003	0.183986664	O
0.686259958	0.243430007	0.148379993	O
0.522770000	0.158970001	0.097186661	O
0.770060013	0.408539987	0.023053360	O
0.975040004	0.347869983	0.135713323	O
0.726549954	0.124389994	0.214593315	O
0.692019958	0.103270000	0.069726690	O
0.942019975	0.353269978	0.047433345	O
0.812030011	0.417739973	0.169439983	O
0.550429955	0.174409995	0.191160011	O
0.124400017	0.971769999	0.117846680	O
0.369720032	0.720099978	0.001059977	O
0.375360066	0.535979965	0.110753314	O
0.129689990	0.822200003	0.223353354	O
0.060910014	0.508829986	0.037660027	O

0.310909983	0.758830020	0.079500008	O
0.454730091	0.015110000	0.183979988	O
0.186269986	0.743429999	0.148379993	O
0.022770017	0.658969956	0.097186661	O
0.270059986	0.908539905	0.023053360	O
0.475049980	0.847880016	0.135713323	O
0.226549993	0.624379965	0.214593315	O
0.192019987	0.603269974	0.069726690	O
0.442020000	0.853269970	0.047433345	O
0.312039971	0.917739966	0.169446659	O
0.050419959	0.674409987	0.191160011	O
0.624400042	0.971780002	0.117853292	O
0.869719997	0.720099978	0.001059977	O
0.875360006	0.535969963	0.110753314	O
0.629699994	0.822200003	0.223353354	O
0.560910014	0.508829986	0.037660027	O
0.810909993	0.758820017	0.079500008	O
0.954729986	0.015110000	0.183979988	O
0.686259983	0.743429999	0.148379993	O
0.522769999	0.658969956	0.097186661	O
0.770060056	0.908539905	0.023053360	O
0.975039976	0.847880016	0.135713323	O
0.726549958	0.624379965	0.214593315	O
0.692019987	0.603269974	0.069726690	O
0.942020000	0.853269970	0.047433345	O
0.812029967	0.917739966	0.169446659	O
0.550419977	0.674409987	0.191160011	O
0.811097314	0.445240015	0.336145751	Ru
0.736824404	0.539201747	0.275285085	Ru
0.764041555	0.599605736	0.376772499	Ru
0.624382447	0.644766892	0.323453426	Ru
0.510108414	0.537319181	0.314406649	Ru
0.647415093	0.404479847	0.293647385	Ru
0.644130008	0.493239987	0.367869409	Ru

BiPO₄
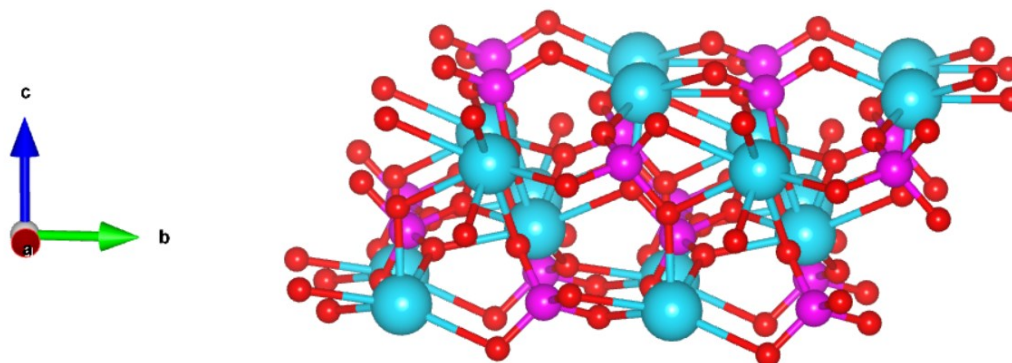
The lattice vector (Å) of the structural model.

a	13.7	0.0	0.0
b	3.2	12.7	0.0
c	0.0	0.0	30.0

Table S6. Atomic coordinates for pristine for Ru/BiPO₄

0.106959993	0.292569983	0.083633359	Bi
0.356960013	0.042569996	0.033526675	Bi
0.393310039	0.204939996	0.147513358	Bi
0.143360011	0.488999983	0.193946679	Bi
0.606959958	0.292569983	0.083633359	Bi
0.856959944	0.042569996	0.033526675	Bi
0.893299827	0.204939996	0.147520002	Bi
0.643359993	0.488999983	0.193946679	Bi
0.106959979	0.792569994	0.083633359	Bi
0.356960001	0.542569998	0.033526675	Bi
0.393299982	0.704940026	0.147520002	Bi
0.143370013	0.989000013	0.193946679	Bi
0.606959979	0.792569994	0.083633359	Bi
0.856959967	0.542569998	0.033526675	Bi
0.893299818	0.704930024	0.147513358	Bi
0.643369944	0.989000013	0.193946679	Bi
0.101090001	0.055829995	0.079606628	P
0.351090013	0.305829996	0.037553342	P
0.403189990	0.454919987	0.150979996	P
0.146649996	0.220249991	0.196239980	P
0.601089897	0.055829995	0.079606628	P
0.851089908	0.305829996	0.037553342	P

29

0.903190025	0.454910022	0.150979996	P
0.646659999	0.220249991	0.196239980	P
0.101089986	0.555830011	0.079606628	P
0.351089999	0.805830007	0.037553342	P
0.403190006	0.954920017	0.150979996	P
0.146649987	0.720240018	0.196239980	P
0.601089986	0.555830011	0.079606628	P
0.851089999	0.805830007	0.037553342	P
0.903189999	0.954909939	0.150979996	P
0.646659991	0.720240018	0.196239980	P
0.124399982	0.471780009	0.117853292	O
0.369720037	0.220100005	0.001059977	O
0.375360069	0.035980001	0.110753314	O
0.129700005	0.322189970	0.223359998	O
0.060910005	0.008830000	0.037660027	O
0.310909997	0.258830008	0.079500008	O
0.454730034	0.515120008	0.183979988	O
0.186259987	0.243439991	0.148379993	O
0.022770000	0.158970001	0.097186661	O
0.270060013	0.408539987	0.023053360	O
0.475050032	0.347879986	0.135713323	O
0.226560027	0.124389994	0.214593315	O
0.192020027	0.103270000	0.069726690	O
0.442020009	0.353269978	0.047433345	O
0.312030011	0.417739973	0.169446659	O
0.050429998	0.174409995	0.191160011	O
0.624400070	0.471769969	0.117853292	O
0.869719967	0.220100005	0.001059977	O
0.875360183	0.035969998	0.110753314	O
0.629700177	0.322200011	0.223359998	O
0.560909987	0.008830000	0.037660027	O
0.810910046	0.258819987	0.079500008	O
0.954729984	0.515100003	0.183986664	O
0.686259958	0.243430007	0.148379993	O
0.522770000	0.158970001	0.097186661	O
0.770060013	0.408539987	0.023053360	O
0.975040004	0.347869983	0.135713323	O
0.726549954	0.124389994	0.214593315	O
0.692019958	0.103270000	0.069726690	O
0.942019975	0.353269978	0.047433345	O
0.812030011	0.417739973	0.169439983	O
0.550429955	0.174409995	0.191160011	O
0.124400017	0.971769999	0.117846680	O
0.369720032	0.720099978	0.001059977	O
0.375360066	0.535979965	0.110753314	O
0.129689990	0.822200003	0.223353354	O
0.060910014	0.508829986	0.037660027	O
0.310909983	0.758830020	0.079500008	O
0.454730091	0.015110000	0.183979988	O

0.186269986	0.743429999	0.148379993	O
0.022770017	0.658969956	0.097186661	O
0.270059986	0.908539905	0.023053360	O
0.475049980	0.847880016	0.135713323	O
0.226549993	0.624379965	0.214593315	O
0.192019987	0.603269974	0.069726690	O
0.442020000	0.853269970	0.047433345	O
0.312039971	0.917739966	0.169446659	O
0.050419959	0.674409987	0.191160011	O
0.624400042	0.971780002	0.117853292	O
0.869719997	0.720099978	0.001059977	O
0.875360006	0.535969963	0.110753314	O
0.629699994	0.822200003	0.223353354	O
0.560910014	0.508829986	0.037660027	O
0.810909993	0.758820017	0.079500008	O
0.954729986	0.015110000	0.183979988	O
0.686259983	0.743429999	0.148379993	O
0.522769999	0.658969956	0.097186661	O
0.770060056	0.908539905	0.023053360	O
0.975039976	0.847880016	0.135713323	O
0.726549958	0.624379965	0.214593315	O
0.692019987	0.603269974	0.069726690	O
0.942020000	0.853269970	0.047433345	O
0.812029967	0.917739966	0.169446659	O
0.550419977	0.674409987	0.191160011	O

References for supporting information:

1 G.Kresse, J. H., Ab initio molecular dynamics for liquid metals. *Phys. Rev. B: Condens. Matter* **1993,** *47* (1), 558-561.

2 G. Kresse, J. F., Efficiency of ab-initio total energy calculations for metals and semiconductors using a plane-wave basis set. *Comput. Mater. Sci.* **1996,** *6* (1), 15-50.

3 G. Kresse, D. J., From ultrasoft pseudopotentials to the projector augmented-wave method. *Phys. Rev. B* **1999,** *59* (3), 1758-1775.

4 Nørskov, J. K., Bligaard, T., Logadottir, A., Kitchin, J. R., Chen, J. G., Pandelov, S., Stimming, U., Trends in the Exchange Current for Hydrogen Evolution. *J. Electrochem. Soc.* **2005,** *152* (3), J23-J26.

5 Li, W.; Liu, Y.; Wu, M.; Feng, X.; Redfern, S. A. T.; Shang, Y.; Yong, X.; Feng, T.; Wu, K.; Liu, Z.; Li, B.; Chen, Z.; Tse, J. S.; Lu, S.; Yang, B., Carbon Quantum Dots Loaded Ruthenium Nanoparticles as an Efficient Electrocatalyst for Hydrogen Production in Alkaline Media. *Adv. Mater.* **2018,** *30* (31), e1800676.

6 He, Q.; Tian, D.; Jiang, H.; Cao, D.; Wei, S.; Liu, D.; Song, P.; Lin, Y.; Song, L., Achieving Efficient Alkaline Hydrogen Evolution Reaction over a Ni_5P_4 Catalyst Incorporating Single-Atomic Ru Sites. *Adv. Mater.* **2020,** *32* (11), e1906972.

7 Liu, Y. L., S.Wang, Y. Zhang, Q. Gu, L. Zhao, S. Xu, D. Li, Y. Bao, J. Dai, Z., Ru Modulation Effects in the Synthesis of Unique Rod-like $Ni@Ni_2P$-Ru Heterostructures and Their Remarkable Electrocatalytic Hydrogen Evolution Performance. *J Am. Chem. Soc.* **2018,** *140* (8), 2731-2734.

8 Qin, Q.; Jang, H.; Chen, L.; Nam, G.; Liu, X.; Cho, J., Low Loading of Rh_xP and RuP on N, P Codoped Carbon as Trifunctional Electrocatalysts for the Oxygen and Hydrogen Electrode Reactions. *Adv. Energy Mater.* **2018,** *8* (29), 1801478.

9 Lu, B.; Guo, L.; Wu, F.; Peng, Y.; Lu, J. E.; Smart, T. J.; Wang, N.; Finfrock, Y. Z.; Morris, D.; Zhang, P.; Li, N.; Gao, P.; Ping, Y.; Chen, S., Ruthenium atomically dispersed in carbon outperforms platinum toward hydrogen evolution in alkaline media. *Nat. Commun.* **2019,** *10* (1), 631.

10 Li, F.; Han, G. F.; Noh, H. J.; Ahmad, I.; Jeon, I. Y.; Baek, J. B., Mechanochemically Assisted Synthesis of a Ru Catalyst for Hydrogen Evolution with Performance Superior to Pt in Both Acidic and Alkaline Media. *Adv. Mater.* **2018,** *30* (44), e1803676.

11 Mao, J.; He, C. T.; Pei, J.; Chen, W.; He, D.; He, Y.; Zhuang, Z.; Chen, C.; Peng, Q.; Wang, D.; Li, Y., Accelerating water dissociation kinetics by isolating cobalt atoms into ruthenium lattice. *Nat. Commun.* **2018,** *9* (1), 4958.

12 Liang, J.; Zhu, L.; Chen, S.; Priest, C.; Liu, X.; Wang, H. L.; Wu, G.; Li, Q., Defect-Rich Copper-doped Ruthenium Hollow Nanoparticles for Efficient Hydrogen Evolution Electrocatalysis in Alkaline Electrolyte. *Chem. Asian. J.* **2020,** *15,* 1-6.

13 Chen, C. H.; Wu, D.; Li, Z.; Zhang, R.; Kuai, C. G.; Zhao, X. R.; Dong, C. K.; Qiao, S. Z.; Liu, H.; Du, X. W., Ruthenium-Based Single-Atom Alloy with High Electrocatalytic Activity for Hydrogen Evolution. *Adv. Energy Mater.* **2019,** *9* (20), 1803913.

14 Wang, Z. L.; Sun, K.; Henzie, J.; Hao, X.; Li, C.; Takei, T.; Kang, Y. M.; Yamauchi, Y., Spatially Confined Assembly of Monodisperse Ruthenium Nanoclusters in a Hierarchically Ordered Carbon Electrode for Efficient Hydrogen Evolution. *Angew. Chem. Int. Ed.* **2018,** *57* (20), 5848-5852.

15 Li, P.; Duan, X.; Wang, S.; Zheng, L.; Li, Y.; Duan, H.; Kuang, Y.; Sun, X., Amorphous Ruthenium-Sulfide with Isolated Catalytic Sites for Pt-Like Electrocatalytic Hydrogen Production Over Whole pH Range. *Small* **2019,** *15* (46), e1904043.